

EFSUMB

European Federation of Societies for Ultrasound in Medicine and Biology



EFSUMB Course Book

2nd Edition

Editor: Christoph F. Dietrich

Ch05: Musculoskeletal Ultrasound

Giorgio Tamborrini¹, Christian Dejaco² and Peter Mandl³

1. Ultrasound Center Basel, Switzerland.

2. Hospital Brunico-Bruneck, Brunico, Italy and Medical University Graz, Graz, Austria.

3. Medical University of Vienna, Vienna, Austria.

Corresponding author: KD Dr. med. Giorgio Tamborrini

Ultrasound Center Basel and Zürich, Aeschenvorstadt 58, 4051 Basel Switzerland

Tel.: (+) 41 61 225 1010

Email: gt@uzrbasel.ch

Web: www.rheuma.com

Introduction

Ultrasound is a validated, excellent imaging tool for the diagnosis and assessment of musculoskeletal (MSK) diseases, and in particular inflammatory and non-inflammatory joint diseases. Musculoskeletal ultrasound (MSK US) plays an important role in visualising both soft tissue structures as well as cartilage and bone, and can detect a variety of pathological changes. In rheumatological practice linear transducers are predominantly utilised. Generally used frequencies range between 5 MHz and 22 MHz, depending on the tissue or joint under investigation. MSK structures are assessed dynamically in real-time and statically with the advantage of multiplanar views. Furthermore, MSK US is a useful tool to guide interventions in the MSK system. Limitations of this technique include limited acoustic windows, difficulty in detecting pathology in large/deep joints, limited view and operator experience.

Anatomy

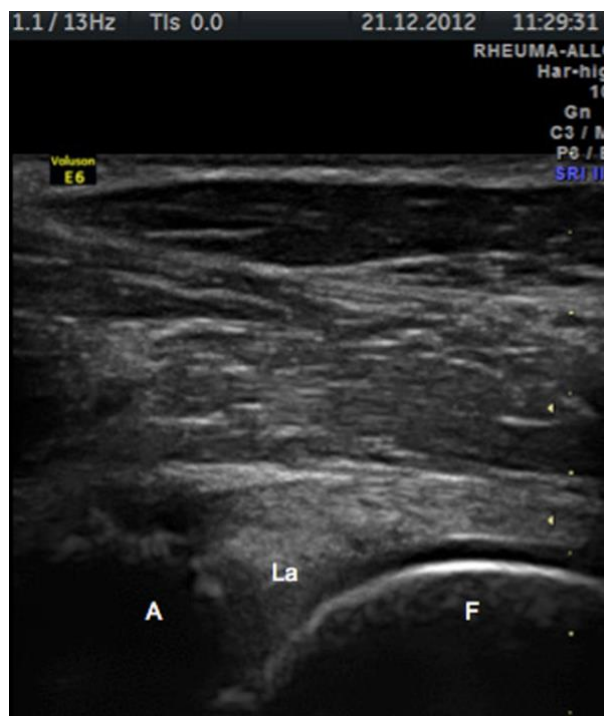
MSK structures have different echogenicity and therefore different degrees of reflectivity that determine their specific MSK US appearance. In this chapter, ultrasound patterns of normal MSK tissues are discussed [1-5].

Cartilage

In the MSK system we primarily visualise two types of cartilage, hyaline cartilage and fibrocartilage. Typical examples of fibrocartilage are the triangular fibrocartilage complex (TFCC) of the wrist [Figure 1], the menisci of the knee [Figure 2], the labrum of the hip [Figure 3] or the labrum of the glenohumeral joint. A small fibrous cartilage layer also lies at the insertions of ligaments or tendons onto bone as part of fibrocartilaginous entheses. Normal fibrocartilage appears iso- to hyperechoic depending on the insonation angle.

Figure 1 Triangular fibrocartilage complex of the wrist. Extensor carpi ulnaris tendon (ECU); ulna (UI); triangular fibrocartilage complex (TFCC).



Figure 2 Meniscus of the knee. Femur (F); meniscus (Me); tibia (T).**Figure 3 Labrum of the hip. Labrum (La); acetabulum (A); femur (F).**

Hyaline cartilage can be assessed in almost all accessible joints. Hyaline articular cartilage can be visualised as a sharp anechoic band (using low gain) coating the bony cortex. Normal hyaline cartilage is homogeneous, regular and has continuous margins. The hyaline cartilage can be well separated from the overlying soft tissue by a hyperechoic interface. Another hyperechoic interface is found between the cartilage and the subchondral bony cortex [Figure 4].

Figure 4 Articular cartilage of the finger joint. Hyaline articular cartilage (aC); metacarpal head (MCH); interfaces (>).



Bone

In assessing bone structure, one of the limitations of MSK US becomes apparent; the bright bony cortex reflects most US waves and appears as a hyperechoic structure. This leads to a limited acoustic window and therefore a limited acoustic view. This is due to the higher acoustic impedance of bone compared to adjacent soft tissue. Visualising structures deep to the bony cortex, such as bone marrow is therefore not possible [Figures 5 and 6]. Generally, we are unable to visualise the normal periosteum.

Figure 5 Bone. Hyperechoic bone surface of the metacarpal head (arrows).

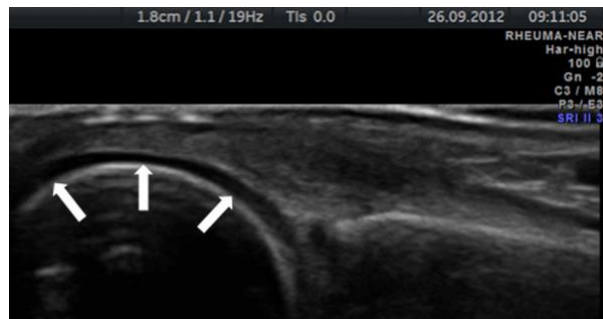
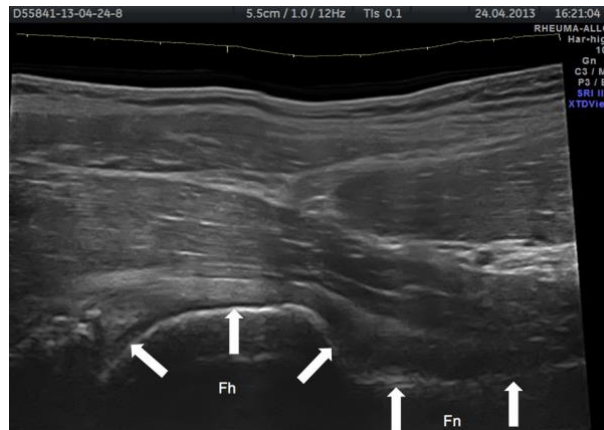


Figure 6 Bone. Hyperechoic bone surface of the femur (arrows); femoral head (Fh); femoral neck (Fn).



Tendons and ligaments

Tendons and ligaments of joints appear as hyperechoic linear structures with echogenic fibrils corresponding to endo- and peritendineal septa [Figure 7]. Depending on the insonation angle, tendons and ligaments change their echogenicity from hyper- to hypoechoic [Figure 8]. This phenomenon is called anisotropy and can be used to identify structures with this property within challenging anatomical areas. Examples include distinguishing the median nerve from the flexor tendons in the volar wrist and assessing the semimembranosus tendon and the tendon of the medial head of the gastrocnemius muscle in the popliteal fossa, when searching for a Baker's cyst.

Figure 7 Flexor tendons of the finger. Hyperechoic deep flexor tendon (dFT); hyperechoic superficial flexor tendon (sFT); A1 pulley (pu); volar plate (vP).



Figure 8 Anisotropy in the biceps tendon: hyperechoic appearance when the insonation angle is 90 degrees (arrow head in the left image) or hypoechoic appearance when changing the angle (arrow head in the right image).



Muscles

Typically, muscles have a hypoechoic pattern. In old age, the echotexture of muscle becomes more echoic due to loss of water, atrophy and progressive fatty infiltration. When a muscle is scanned in the transverse plane, several echoic to hyperechoic dots can be seen corresponding to endo-, peri- and epimysium. In the longitudinal view we can visualise these as parallel and oblique echoic fibres [Figure 9].

Figure 9 Hypoechoic deltoid muscle on transverse view and on longitudinal view with parallel and oblique echoic fibres. Deltoid muscle on transverse view (DMt); deltoid muscle on longitudinal view (DMI); biceps tendon (Bi).



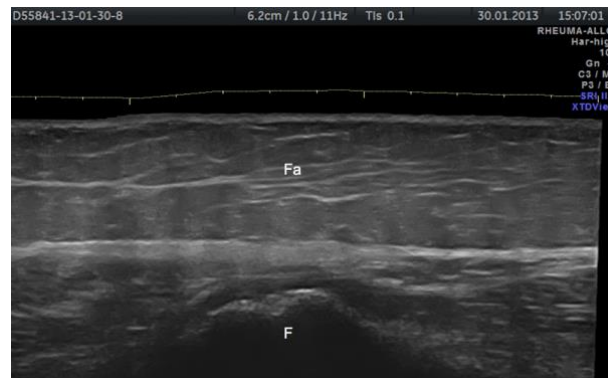
Skin and fat

Using high frequency transducers (18 to 60 MHz) the skin appears as a hyperechoic band [Figure 10], whilst subcutaneous fat appears as a hypoechoic lobulated structure with iso- or hyperechoic connective tissue fibres [Figure 11].

Figure 10 Skin. Skin (Sk); flexor tendons (FT); metacarpal head (Mc).



Figure 11 Hypoechoic fat at the lateral hip. Subcutaneous fat (Fa); femur (F).



Nerves and vessels

Using high frequency transducers we can see peripheral nerves [Figure 12]. Typically we see linear hypoechoic fascicles surrounded by the hyperechoic endoneurium and perineurium. The epineurium of a nerve appear as parallel hyperechoic band. Blood vessels appear as anechoic compressible tubular structures (longitudinal view) or as round structures (transverse view) [Figure 12].

Figure 12 Median nerve at the level of the wrist. Median nerve (MN); ulnar artery (UA).



Synovium and bursa

Normally the synovial lining of a joint, bursa or tendon sheath can be seen as a fine iso- to hyperechoic line with a small amount of hypoechoic synovial fluid [Figure 13]. The fluid is displaceable. A small amount of physiological fluid inside a bursa can be found for example in the retrocalcaneal bursa [Figure 14] or in the deep infrapatellar bursa.

Figure 13 Synovial recess of the proximal interphalangeal finger joint. Flexor tendons (Ft); synovial recess (Sy); volar plate (vP); head of the proximal phalanx (Ph).



Figure 14 Retrocalcaneal bursa. Hypoechoic fluid inside the bursa (Bu); calcaneus (Ca); achilles tendon (AT).



Examination technique

The patient has to be in the correct position for the anatomical region of interest to make the examination comfortable both for the patient and for the examiner. The position of the patient and the standard scan techniques depend on the area under investigation. For example, when examining the shoulder joint the patient is placed in a sitting position and at the beginning of the examination it is preferred to flex the elbow joint to 90°, with the hand is positioned in supination on top of the patient's thigh to scan the posterior or anterior structures. For dynamic assessment, active and passive external and internal rotation of the humerus is additionally performed. When examining the hip joint, the patient is scanned in a supine position whilst the hip joint stays in a neutral position. Generally, all structures are assessed in longitudinal and transverse scans. Optional oblique or unconventional views are added to perform additional in-depth assessment of specific musculoskeletal structures. A further helpful characteristic of MSK US is that we are able to dynamically assess structures, for example whilst keeping the transducer static, joints can be assessed in various positions, providing additional functional information. This technique permits assessment of a structure in a static and dynamic way through active, passive or resisted movement with the advantage of direct anatomical and functional visualisation. Moreover, MSK US-guided interventions may be performed such as diagnostic synovial fluid aspiration or therapeutic injection. The structures should be scanned bilaterally and compared to increase diagnostic certainty.

VIP: very important pathologies in the MSK system

Cartilage pathology

Primary or secondary (e.g. post-traumatic) osteoarthritis (OA) is one of the most frequent MSK pathologies. In early disease we find a loss of sharpness, homogeneity and anechogenicity of the articular cartilage. Furthermore, we see irregular interfaces of the overlying soft tissue and of the subchondral bone and finally, focal or diffuse thinning of the

hyaline articular cartilage [Figure 15]. These findings are not specific for OA, for example, similar changes can also be found in one of the most frequent inflammatory rheumatic diseases, namely rheumatoid arthritis (RA).

In crystal deposition diseases, specific pathological findings of the hyaline cartilage are present. In gout, monosodium urate crystals (MSU) may be visualised as a hyperechoic diffuse or focal enhancement of the superficial margin of the hyaline articular cartilage ('double contour' sign) [Figure 16]. In calcium pyrophosphate deposition disease (CPPD) hyperechoic dots or lines inside the hyaline articular cartilage are typically found [Figure 17]. The same findings may occur in fibrocartilage, e.g. in the meniscus, labrum, wrist [Figure 18] or symphysis. Degenerated or injured fibrocartilage can appear inhomogeneous. In meniscal degeneration, such as in OA, the meniscus is extruded and parameniscal ganglion cysts may be visualised [Figure 19] [6, 7].

Figure 15 Osteoarthritis of the knee. Normal cartilage of the femoral condyles (Ca); thinning of the cartilage (>).

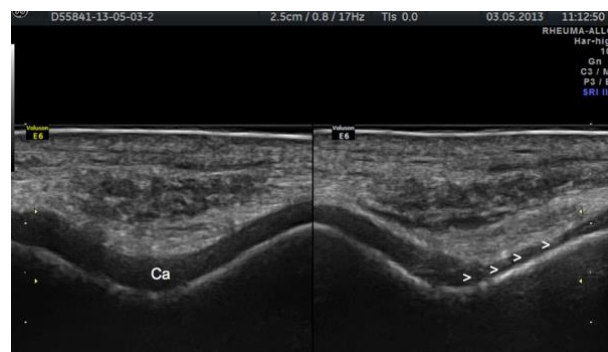


Figure 16 Gout in the first metatarsal joint. Hyperechoic soft tissue calcification (C); metatarsal head (Mt); double contour sign (>).



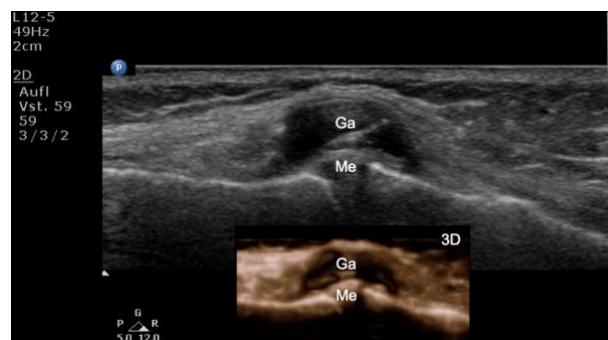
Figure 17 Calcium pyrophosphate dihydrate deposition disease in the knee. Cartilage of the femoral condyle (Ca); hyperechoic calcifications inside the hyaline cartilage (>).



Figure 18 Calcium pyrophosphate dihydrate deposition disease of the wrist. Ulna (UI); calcifications of the TFCC (Ca); extensor carpi ulnaris tendon (ECU).



Figure 19 Parameniscal ganglion. Ganglion (Ga); meniscus (Me).



Bone pathology

Bony overgrowths, also known as osteophytes are a typical characteristic of degenerative joint disease and osteoarthritis (OA). Osteophytes appear in MSK US as hyperechoic step-up

lesions of the bony cortex [Figure 20]. Osteophytes can also be found in inflammatory joint diseases such as psoriatic arthritis (PsA) or in end-stage RA. Erosions of the bone are typical in erosive RA [Figure 21] but also in erosive osteoarthritis (eOA). An erosion is defined as an intra-articular discontinuity of the bone surface that is visible in two perpendicular planes. Another example of bone pathology that can be assessed is fractures, seen as a discontinuity of the bony cortex and sometimes visible bulging of hyperechoic periosteum due to a hyperechoic or anechoic haematoma [Figure 22] [8].

Figure 20 Osteoarthritis of the knee. Femur (F); osteophytes (Op); tibia (T).



Figure 21 Erosion of the metacarpal head in RA. Normal metacarpal head (Mc); erosion (E).

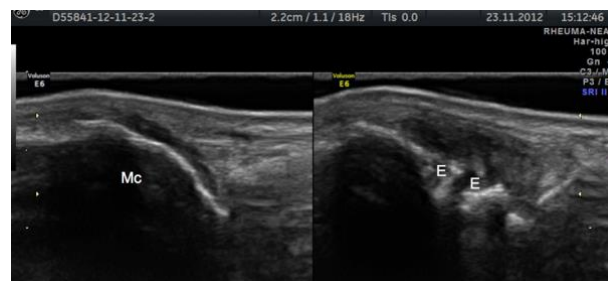
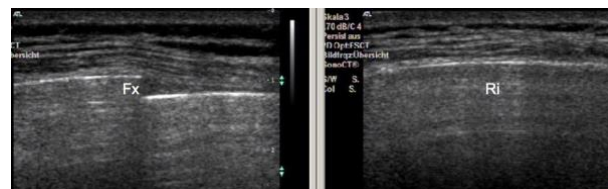


Figure 22 Rib fracture. Fracture (Fx); normal rib (Ri).



Pathology of tendons and ligaments

Tendons and joint ligaments can be injured by mechanical overloading or trauma. Tendon degeneration (tendinosis) is frequent, for example in the Achilles tendon [Figure 23, 24 and 25], proximal patellar tendon or in the rotator cuff of the shoulder or the hip [Figure 26]. Partial or full thickness tears may occur [Figure 27]. In tendinosis, calcium deposition inside the tendons or ligaments is often found [Figure 28]. The calcium deposits can penetrate the bone or the bursa and cause inflammation and pain. Crystal deposition in tendons and ligaments is common in inflammatory crystal deposition diseases such as calcium pyrophosphate dihydrate deposition disease (CPPD) or gout [Figure 29].

The insertion of ligaments and tendons into the bones are called entheses. In mechanical overloading and in inflammatory diseases (for example in peripheral spondyloarthritis (pSpA)), inflammatory signs (thickening of the tendon, abnormal hypoechoic zones in the tendon, tendon calcification, bursitis, increased vascularisation within a 2 mm zone of the bony cortex) and post-inflammatory signs (bony overgrowth occurring in the entheses (enthesophytes), irregular bone surface and erosions, especially in pSpA) can be found [Figure 30]. Modern techniques to assess stiffness and inflammation are elastosonography and 3D/4D-scans. Tenosynovitis is discussed in the section 'Pathology of synovia and bursae' [9-11].

Figure 23 Achilles tendon tendinosis. Thickened achilles tendon (Te); calcaneus (Ca).

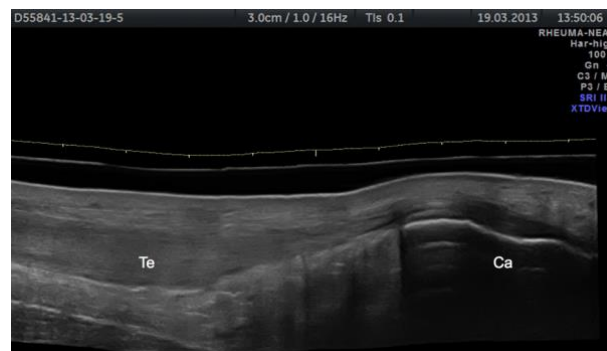


Figure 24 Achilles tendon full thickness tear. Tear (><); calcaneus (Ca).

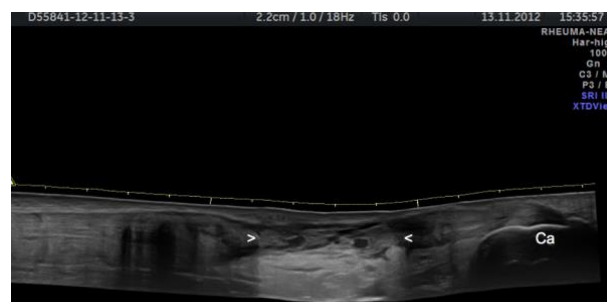


Figure 25 Achilles tendon tendinosis with increased vascularisation, 3D power Doppler scan. Transverse view (A); longitudinal view (B); coronal view (C); 3D view (3D).

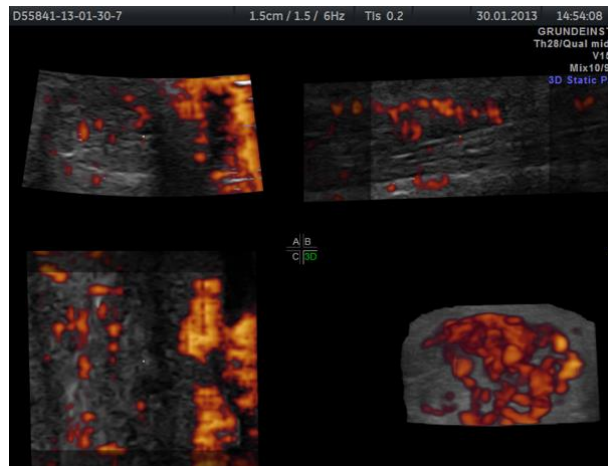


Figure 26 Tendinosis of the supraspinatus tendon. Humerus (Hu); inhomogeneous thickened tendon (Te).



Figure 27 Full thickness tear of the supraspinatus tendon. Humerus (Hu); tendon tear filled with anechoic fluid (Te).

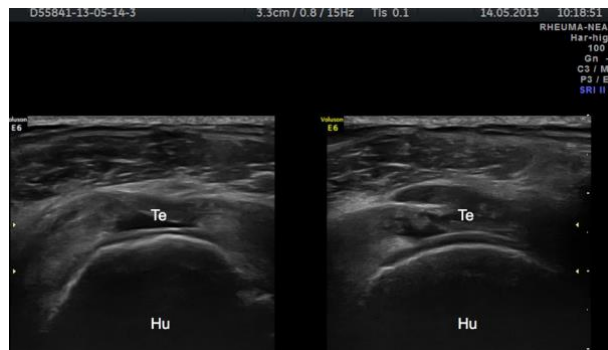


Figure 28 Calcification of the supraspinatus tendon. Hyperechoic calcium deposits in the tendon with acoustic shadowing (Ca).

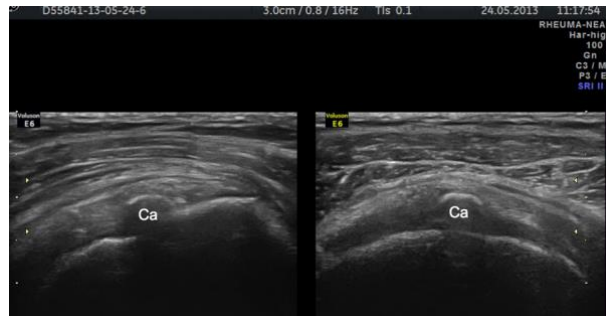


Figure 29 Achilles tendon calcification. Achilles tendon (AT); hyperechoic calcification (>); bony enthesophyte of the calcaneus (Ep).



Figure 30 Enthesitis in spondyloarthritis. Irregular bony cortex of the calcaneus (Ca); pathological vascularisation of the achilles tendon (>).



Muscle pathology

MSK US is an excellent tool for the diagnosis of muscle tears [Figure 31]. We can visualise haematomas (early assessment shows a hyperechoic pattern, later changing to a hypoechoic pattern) [Figure 32] and see a loss of the normal architecture. In inflammatory diseases, (e.g. myositis) we can see hypoechoic oedema or hyperechoic ectopic calcifications in muscle.

Whenever muscles or other soft tissues are scanned, a comparison with the other side should be performed [6].

Figure 31 Partial tear of the deltoid muscle on a transverse view, left image showing the normal deltoid muscle on the other side. Deltoid muscle (Dm); tear (>); subscapularis tendon (SuT).

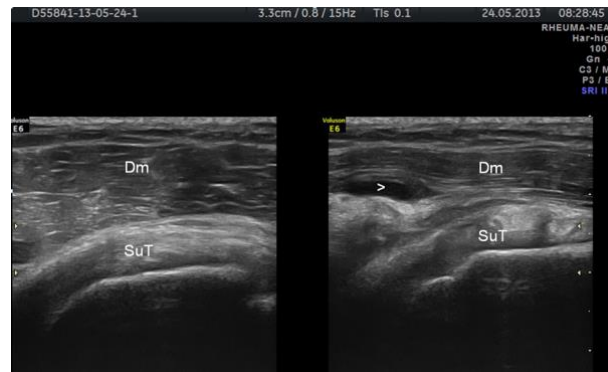
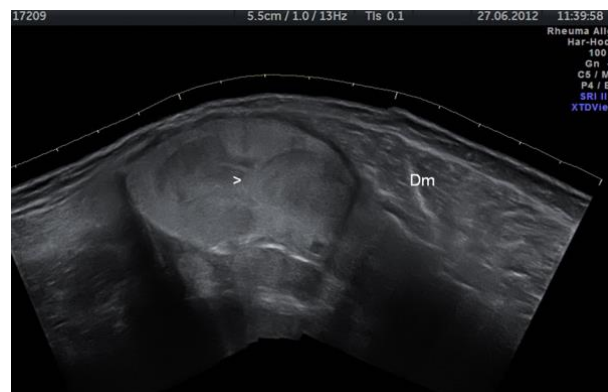


Figure 32 Haematoma and tear of the deltoid muscle on extended transverse view. Deltoid muscle (Dm); hyperechoic haematoma (>).



Pathology of skin and fat

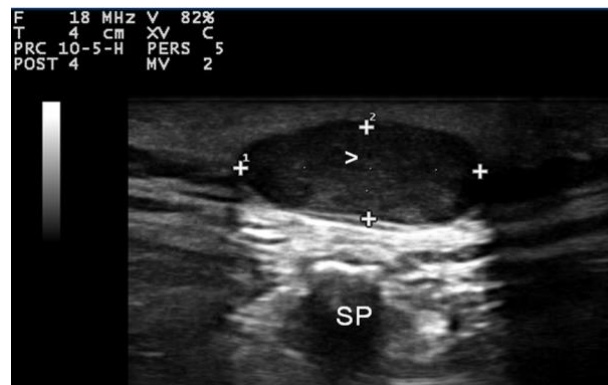
Typical rheumatic diseases involving the skin are connective tissue diseases (for example dermatomyositis, systemic lupus erythematosus, systemic sclerosis) or psoriatic arthritis (PsA). In these diseases, by using very high frequency transducers (> 22MHz and up to 60 MHz) we can see an increased thickness or vascularisation of the affected skin. Even the nail in PsA can be scanned to assess texture irregularities, inflammation of the nail matrix and simultaneous enthesitis of the enclosed tendons and ligaments [Figure 33]. Another technique to determine the elasticity and stiffness of the skin (for example in systemic sclerosis) is elastography, which is beyond the scope of this chapter. Moreover, MSK US is an excellent tool to visualise foreign bodies or abscesses in the skin and subcutaneous tissue. A

common pathology of fatty tissue are benign tumours known as lipomas. The typical appearance is hyperechoic compared to the surrounding hypoechoic fat [Figure 34] [12,13].

Figure 33 Distal interphalangeal joint in PsA. Thickened skin (>); erosion (Er); increased vascularisation at the insertion of the extensor tendon and nail matrix (Nm).



Figure 34 Lipoma. Subcutaneous lipoma (> and +), spinous process (SP).



Pathology of nerves and vessels

High resolution nerve ultrasound allows us to visualise different nerve pathologies, for example nerve tumours like schwannomas or neuromas. Common entrapment sites are the carpal tunnel (median nerve) or the tarsal tunnel (posterior tibial nerve). In carpal tunnel syndrome we can usually visualise a thickened and hypoechoic nerve proximal to the site of compression [Figure 35]. Sometimes, increased vascularisation inside the compressed nerve can be detected and restricted movement of the nerve is seen with flexion/extension of the fingers. In large vessel vasculitis, for example in giant cell arteritis, we can see a stenosis of the artery with a pathological compression sign and an increased thickness of the vessel wall generating a 'halo' [Figure 36] [14].

Figure 35 Carpal tunnel syndrome. Thickened median nerve (MN); flexor carpi radialis tendon (Fcr); flexor pollicis longus tendon (Fpl).



Figure 36 Giant cell arteritis. Stenosis of the temporal artery in a 3D power Doppler mode (arrows); anechoic halo in a transverse view (><).



Pathology of synovia and bursae

The definitions of synovial fluid, synovial hypertrophy and tenosynovitis according to definitions of OMERACT Ultrasound Working Group are listed in Table 1 [15].

Table 1 OMERACT 7 definitions.

Synovial Fluid	Abnormal hypoechoic or anechoic (relative to subdermal fat, but sometimes may be isoechoic or hyperechoic) intra-articular material that is displaceable and compressible, but does not exhibit Doppler signal.
Synovial Hypertrophy	Abnormal hypoechoic (relative to subdermal fat, but sometimes may be isoechoic or hyperechoic) intra-articular tissue that is non-displaceable and poorly compressible and which may exhibit Doppler signal.
Tenosynovitis	Hypoechoic or anechoic thickened tissue with or without fluid within the tendon sheath, which is seen in 2 perpendicular planes and which may exhibit Doppler signal.

Synovial effusions can occur in OA [Figure 37 and 38] and more often in inflammatory joint diseases such as RA [Figure 39 and 40], crystal deposition diseases, infections or spondyloarthritis. Table 2 shows the typical MSK US findings in OA compared to RA. MSK US is a valuable tool in the monitoring of disease progression and in the assessment of response to local and systemic treatment, helping rheumatologists in the clinical management of patients.

Table 2 MSK US findings in osteoarthritis compared to rheumatoid arthritis

Tissue	Osteoarthritis	Rheumatoid arthritis
Joint/bursa/tendon	<ul style="list-style-type: none"> - joint effusion - synovial hypertrophy and hyperaemia - joint capsule thickening - bursitis - meniscal tears, meniscal extrusion 	<ul style="list-style-type: none"> - joint effusion - synovial hypertrophy and hyperaemia invading the bone erosions - joint capsule thickening - bursitis, tenosynovitis, rheumatoid nodules, tendon tears, secondary nerve entrapment
Cartilage	<ul style="list-style-type: none"> - loss of sharpness - loss of homogeneity - loss of anechogenicity - irregularities of the anterior and posterior margins - focal or diffuse thinning of the cartilage 	<ul style="list-style-type: none"> - loss of sharpness - loss of homogeneity - loss of anechogenicity - focal or diffuse thinning of the cartilage
Bone	<ul style="list-style-type: none"> - osteophytes - erosions and mucoid cysts especially in erosive finger/hand osteoarthritis 	<ul style="list-style-type: none"> - erosions - secondary osteoarthritic changes, e.g. osteophytes

Synovial membrane thickening and joint effusions can reflect underlying inflammation. There is an association between the amount of damage of the articular cartilage and the degree of conventional radiographic changes. In active inflammatory processes, colour or power Doppler MSK US can demonstrate an increased pannus vascularisation [Figure 41 and 42] and may be predictive of radiographic damage in the course of RA. Contrast enhanced US (CEUS) may improve the measurement of synovial thickness and activity of synovial processes and allows for a more sensitive differentiation between effusion and synovial proliferation. However, this technique is not yet mature nor established in routine practice. In both degenerative and inflammatory joint diseases, bursitis or tenosynovitis may occur [Figure 43 and 44]. In shoulder impingement an inflamed and thickened subdeltoid bursa can be detected [Figure 45]. Tenosynovitis is an early finding in RA [Figure 46] and is also common in crystal deposition disease, mechanical overload or spondyloarthritis [17].

Figure 37 Osteoarthritis of the distal interphalangeal joints. Hypochoic effusion (arrows); osteophytes (>); middle phalanx (mP); distal Phalanx (dP).

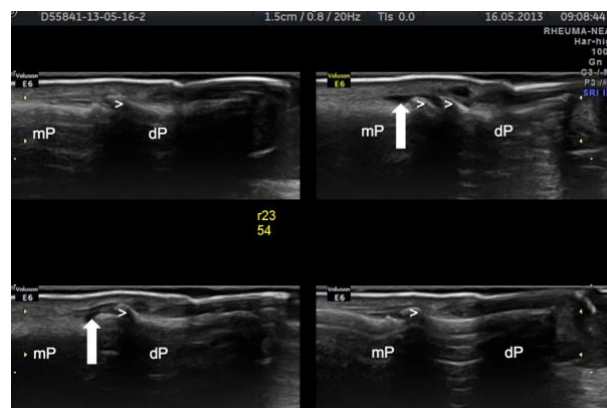


Figure 38 Osteoarthritis of the knee joint. Hypochoic effusion in the suprapatellar recess (arrow); patella (Pa); tibia (Ti).

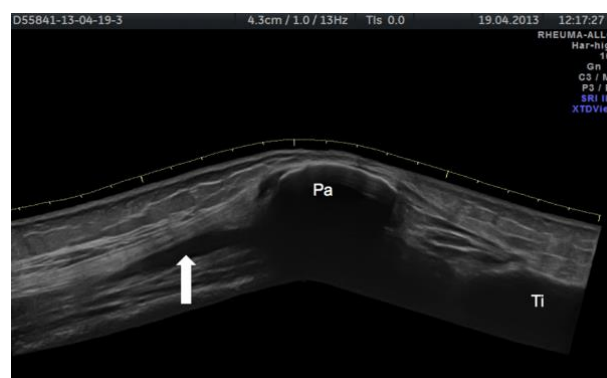


Figure 39 Mild synovial effusion in the metacarpal joint. Hypoechoic effusion in the proximal dorsal recess (arrow); metacarpal head (Mc).



Figure 40 Hypoechoic synovial effusion in the humeroradial elbow joint. Hypoechoic effusion (arrow); lateral condyle of the humerus (Co).



Figure 41 Active synovitis in the metacarpal joint. Increased pannus vascularisation in the power Doppler mode (arrows); metacarpal head (Mc).

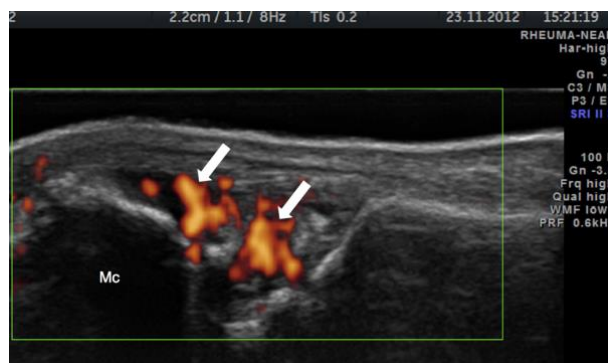


Figure 42 Active synovitis in the radiocarpal joint. Increased pannus vascularisation (power Doppler mode) (arrows); radius (Ra); synovitis (B-Mode) (Sy).

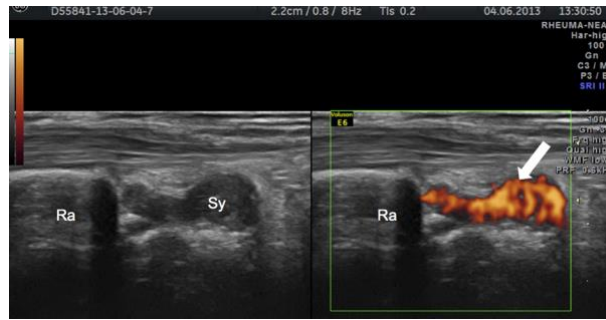


Figure 43 Prepatellar septic bursitis. Hypochoic prepatellar bursitis (arrow); patella (Pa); tibia (Ti).



Figure 44 Gastrocnemius-semimembranosus bursa (Baker's cyst), left image in a transverse view, right image in a longitudinal. Hypochoic bursitis (arrow); medial head of the gastrocnemius muscle (Ga).

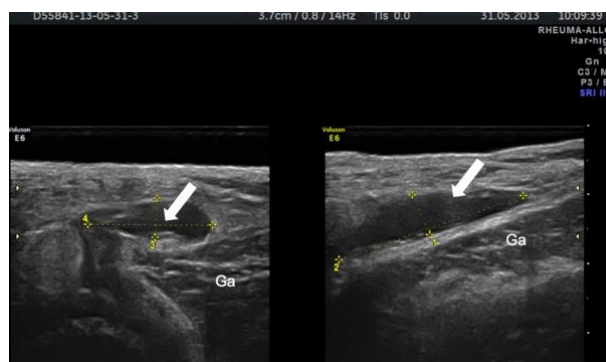
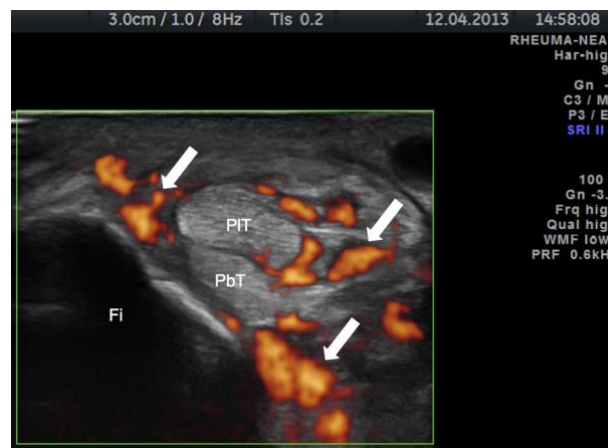


Figure 45 Subdeltoid bursitis. Synovial proliferation (arrows); effusion (>); subscapularis tendon (SuT).



Figure 46 Tenosynovitis. Increased vascularisation in the thickened tendon sheath (arrows); peroneus longus tendon (PIT); peroneus brevis tendon (PbT); fibula (Fi).



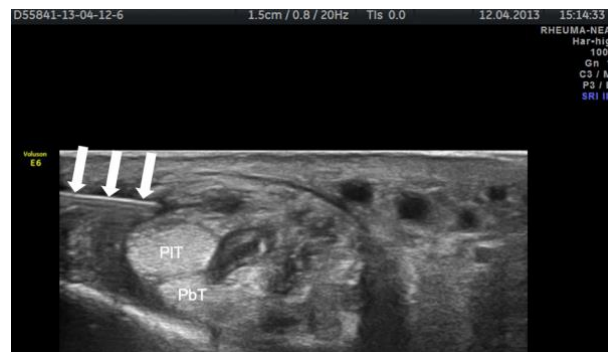
Interventional MSK US

Real time MSK US is a validated useful tool when performing interventions of the MSK system. MSK US helps identify the correct site for needle placement in order to facilitate atraumatic joint aspiration and synovial biopsies. Ultrasound-guided diagnostic and therapeutic interventions are characterised by their excellent accuracy and improved clinical effectiveness compared to unguided procedures [Figure 47 and 48] [16].

Figure 47 Injection in the subdeltoid bursa. Needle (arrows); bursa (Bu); supraspinatus tendon (SpT).



Figure 48 Injection in the tendon sheath of the peroneal tendons near the fibula. Needle (arrows); peroneus longus tendon (PIT); peroneus brevis tendon (PbT).



Summary

In this chapter we present and describe the appearance of various tissues using ultrasound. Deeper structures should be evaluated with low frequency linear probes. When evaluating more superficial tissue or structures, it is better to utilize higher frequencies. Without detailed knowledge of the anatomy of the musculoskeletal system, pathological findings cannot be reliably detected. In addition, one should be familiar with all diseases that can manifest themselves in the musculoskeletal system. In addition to rheumatic diseases, these include other autoimmune diseases, traumatic lesions, orthopaedic or haematological diseases.

References

1. Tamborrini, G., Bruyn GW, Staerkle-Baer A. (2018) Musculoskeletal Ultrasound. Irheuma.com. ISBN 978-3-7460-6295-2

2. Ziswiler, H. and Tamborrini, G. (2011). Ultraschall am Bewegungsapparat I - «Perlen und Kristalle». *Praxis*, 100(21), pp.1289-1295.
3. Ziswiler, H. and Tamborrini, G. (2011). Ultraschall am Bewegungsapparat II oder - wieso Fledermäuse besser sind als Ärzte. *Praxis*, 100(21), pp.1297-1302.
4. Tamborrini, G., Krebs, A., Michel, M., Michel, B. and Ciurea, A. (2011). Webbasierendes Lernen in der Sonographie des Bewegungsapparates. *Zeitschrift für Rheumatologie*, 70(2), pp.154-159.
5. Tamborrini, G., Möller, I., Bong, D., Miguel, M., Marx, C., Müller, A. and Müller-Gerbl, M. (2017). The Rotator Interval – A Link Between Anatomy and Ultrasound. *Ultrasound International Open*, 03(03), pp.E107-E116.
6. Micheroli, R., Kyburz, D., Ciurea, A. and Tamborrini, G. (2011). Die rheumatische Hand - Diagnostik in der Praxis. *Praxis*, 100(18), pp.1097-1106.
7. Filippucci, E., Cipolletta, E., Mashadi Mirza, R., Carotti, M., Giovagnoni, A., Salaffi, F., Tardella, M., Di Matteo, A. and Di Carlo, M. (2019). Ultrasound imaging in rheumatoid arthritis. *La radiologia medica*.
8. Zufferey, P., Brulhart, L., Tamborrini, G., Finckh, A., Scherer, A., Moller, B. and Ziswiler, H. (2014). Ultrasound evaluation of synovitis in RA: Correlation with clinical disease activity and sensitivity to change in an observational cohort study. *Joint Bone Spine*, 81(3), pp.222-227.
9. Sexton, J., Pittman, M. and Morrow, D. (2019). Flexor Tenosynovitis Using Ultrasound. *The Journal of Emergency Medicine*.
10. Docking, S., Cook, J., Chen, S., Scarvell, J., Cormick, W., Smith, P. and Fearon, A. (2019). Identification and differentiation of gluteus medius tendon pathology using ultrasound and magnetic resonance imaging. *Musculoskeletal Science and Practice*, 41, pp.1-5.
11. Krajewska-Włodarczyk, M., Owczarczyk-Saczonek, A., Placek, W., Wojtkiewicz, M., Wiktorowicz, A. and Wojtkiewicz, J. (2019). Distal interphalangeal joint extensor tendon enthesopathy in patients with nail psoriasis. *Scientific Reports*, 9(1).
12. Mlosek, R. and Malinowska, S. (2013). Ultrasound image of the skin, apparatus and imaging basics. *Journal of Ultrasonography*, 13(53), pp.212-221.
13. Tamborrini, G. and Bianchi, S. (2012). Knuckle pads – a rare finding. *Journal of Ultrasonography*, 12(51), pp.493-498.
14. Suk, J., Walker, F. and Cartwright, M. (2013). Ultrasonography of Peripheral Nerves. *Current Neurology and Neuroscience Reports*, 13(2).
15. Zufferey, P., Tamborrini, G., Gabay, C., Krebs, A., Kyburz, D., Michel, B., Moser, U., Villiger, P., So, A. and Ziswiler, H. (2013). Recommendations for the use of ultrasound in rheumatoid arthritis: literature review and SONAR score experience. *Swiss Medical Weekly*.
16. Tamborrini, G., Dejaco, C., Bruyn, G. and Siegenthaler, A. (2019). *Ultrasound and clinically guided Injection techniques on the musculoskeletal system*. 1st ed.irheuma.com, ISBN 978-3-7494-3282-0
17. Balint, PV., Mandl, P. (2018) *Ultrasound of the hand in rheumatology*. Springer, 2018 ISBN-13:978-3319742069